The Journal of Immunology

RESEARCH ARTICLE | DECEMBER 15 2021

Myeloid Cell–Specific IL-4 Receptor Knockout Partially Protects from Adipose Tissue Inflammation FREE

Jan Ackermann; ... et. al

J Immunol (2021) 207 (12): 3081–3089.
https://doi.org/10.4049/jimmunol.2100699

Myeloid Cell–Specific IL-4 Receptor Knockout Partially Protects from Adipose Tissue Inflammation

Jan Ackermann,*,† Lilli Arndt,* Michaela Kirstein,* Constance Hobusch,† Georg Brinker,*,† Nora Klöting,‡,§ Julia Braune,*,†,[1] and Martin Gericke*,†,[1]

IL-4 receptor signaling is supposed to play a major role in anti-inflammatory polarization and proliferation of adipose tissue macrophages. In this study, we examined the metabolic and inflammatory phenotype of C57BL/6J mice (*Il4ra*) with LysM-dependent knockout (*Il4ra*$^{\Delta myel}$) of the IL-4 receptor α-chain (IL-4Rα), the mandatory signaling component of IL-4 and IL-13, on chow and high-fat diet. Lean *Il4ra*$^{\Delta myel}$ mice showed decreased insulin sensitivity, no divergent adipose tissue macrophage polarization, but an increased percentage of CD8$^+$ T cells in visceral adipose tissue. After 20 wk of a high-fat diet, *Il4ra*$^{\Delta myel}$ mice exhibited higher glucose tolerance, no changes in the lymphocyte compartment and fewer M1 macrophages in visceral adipose tissue. In vivo adipose tissue macrophage proliferation measured by BrdU incorporation was unaffected by *Il4ra* knockout. Interestingly, we show that IL-4Rα signaling directly augmented *Itgax* (*Cd11c*) gene expression in bone marrow–derived macrophages and increased the amount of CD11c$^+$ macrophages in adipose tissue explants. Myeloid cell–specific knockout of *Il4ra* deteriorated insulin sensitivity in lean mice but improved parameters of glucose homeostasis and partially protected from adipose tissue inflammation in obese mice. Hence, IL-4Rα signaling probably plays a minor role in maintaining the macrophage M2 population and proliferation rates in vivo. Moreover, our data indicate that IL-4 signaling plays a proinflammatory role in adipose tissue inflammation by directly upregulating CD11c on adipose tissue macrophages. *The Journal of Immunology*, **2021, 207: 3081–3089.**

Obesity is a disease of modern civilizations with a rapidly increasing incidence and a huge number of severe associated diseases that reduce life quality, life expectancy and cause enormous social costs (1–3). It is associated with a higher risk of dying from several infectious diseases, orthopedic problems, cardiovascular disease, and type 2 diabetes (4–6). To fight this threat to global health, it is necessary to address the social circumstances and eating behaviors that lead to the increasing prevalence of obesity as well as to understand the pathophysiology of the associated diseases, to develop effective strategies for prevention and therapy.

The onset of type 2 diabetes is preceded by an increase of proinflammatory leukocytes and cytokines in adipose tissue (AT) (7, 8). Obesity triggers CD8$^+$ T cell infiltration into AT, which in turn seems to channel macrophage accumulation (9). Macrophages play a central role in AT homeostasis because they contribute intensively to the cytokine milieu and their number and metabolic activation in visceral AT is a strong predictor of systemic insulin resistance in obese mice and humans (10, 11). Although there is evidence for a fluent transition between several macrophage activation states, it is helpful to divide macrophage subpopulations into classically activated (M1) macrophages and alternatively activated (M2) macrophages. M1 macrophages produce reactive oxygen and nitrogen species and secrete proinflammatory cytokines, such as TNF-α, IL-1, and IL-12. They can be defined by the expression of the surface marker CD11c. In contrast, M2 macrophages produce high levels of arginase-1 (ARG1), secrete anti-inflammatory cytokines and can be identified by the expression of CD206 or CD301 (12). Because ablation of CD11c$^+$ macrophages improves several metabolic parameters in mice, interfering with the equilibrium between macrophage populations toward an anti-inflammatory M2 state could be a preventative or therapeutic strategy against type 2 diabetes (13, 14).

Systemic IL-4 or IL-13 application in mice has positive effects on lipid and glucose metabolism and both cytokines are frequently used for M2 polarization in vitro and in vivo (15–18). Additionally, we could previously show that IL-4 and IL-13 increase macrophage proliferation in AT ex vivo, which is of concern, because proliferating macrophages contribute to the increase of macrophages in obesity, probably especially to the M2 population (19–21). The

*Institute of Anatomy and Cell Biology, Martin-Luther-University Halle-Wittenberg, Halle, Germany; †Institute of Anatomy, Leipzig University, Leipzig, Germany; ‡Helmholtz Institute for Metabolic, Obesity and Vascular Research of the Helmholtz Zentrum München at the University of Leipzig; and §Medical Department III, Leipzig University, Leipzig, Germany

[1]J.B. and M.G. contributed equally to this work.

ORCIDs: 0000-0002-8424-3215 (J.A.); 0000-0003-2280-1303 (L.A.); 0000-0002-0847-6404 (G.B.); 0000-0002-7625-7254 (N.K.); 0000-0002-0792-5394 (M.G.).

Received for publication July 14, 2021. Accepted for publication October 18, 2021.

This work was supported by the Deutsche Forschungsgemeinschaft (German Research Foundation; Projektnummer 209933838 – Collaborative Research Center (SFB) 1052) (project B1 to M.G., B4 to N.K., and B9 to M.G.) and supported by the Federal Ministry of Education and Research, Germany, Integrated Research and Treatment Center (IFB) AdiposityDiseases 01EO1501. This research work was supported by the research group "SFB1052/2" B1 (to M.G.); B4 (to N.K.) funded by Deutsche Forschungsgemeinschaft and supported by the Federal Ministry of Education and Research, Germany, IFB AdiposityDiseases 01EO1501 (N.K.), German Research Center for Diabetes (82DZD00601), and German Diabetes Association (934300-003) and by a student fellowship to J.A.

J.B. and M.G. designed and established the experiments; J.A., L.A., M.K., C.H., and J.B. performed the experiments; G.B. helped with flow cytometry; N.K. determined the genotypes of the *Il4ra*$^{\Delta myel}$ mouse strain, managed activity measurements, indirect calorimetry, and helped with analytical procedures; and J.A., J.B. and M.G. wrote the manuscript.

Address correspondence and reprint requests to Dr. Martin Gericke at the current address: Institut für Anatomie, Universität Leipzig, Liebigstraße 13, 04103 Leipzig, Germany. E-mail address: martin.gericke@medizin.uni-leipzig.de

The online version of this article contains supplemental material.

Abbreviations used in this article: ARG1, arginase-1; AT, adipose tissue; ATM, adipose tissue macrophage; ATT, AT T cell; BAT, brown adipose tissue; BMDM, bone marrow–derived macrophage; CLS, crown-like structure; HFD, high-fat diet; ipGTT, i.p. glucose tolerance test; ipITT, i.p. insulin tolerance test; M1, classically activated; M2, alternatively activated; PWAT, peritoneal white AT; SWAT, s.c. white AT; YFP, yellow fluorescent protein;

mandatory signaling component for both IL-4 and IL-13 is the IL-4 receptor α-chain (IL-4Rα).

To address the role of IL-4Rα signaling in AT macrophage (ATM) polarization, proliferation, and overall metabolic phenotype in vivo, we investigated lean and obese mice with a conditional *Il4ra* knockout in macrophages. Lean mice with abrogated IL-4Rα signaling in macrophages bore an increased amount of $CD8^+$ lymphocytes in visceral AT and a decreased insulin sensitivity. Obese knockout mice had fewer $CD11c^+$ macrophages in visceral AT and an improved glucose tolerance. Additional evidence suggests a slightly lower level of AT inflammation in obese mice. Counterintuitively, IL-4Rα signaling increased *Itgax* (*Cd11c*) gene expression and the amount of $CD11c^+$ macrophages in vitro and ex vivo and could therefore explain the improved glucose homeostasis in obese myeloid-specific *Il4ra* knockout mice.

Materials and Methods

Animals, research diets, and dissection

All mice were maintained in pathogen-free facilities at the University of Leipzig. Mice lived in groups at 22 ± 2°C on a 12-h light/dark cycle with free access to food and water. Littermates were either fed a regular chow diet (9% kcal fat; Ssniff Spezialdiäten, Soest, Germany) or a high-fat diet (HFD) (60% kcal fat; Ssniff Spezialdiäten) for 20 to 22 wk, starting at the age of 8 wk. Chow mice were euthanized at the age of 18 to 20 wk, whereas HFD mice were euthanized at 30 wk of age. *Il4ra*$^{flx/-}$ mice on C57BL/6J background were a kind gift from Brombacher laboratory (22). *Il4ra*$^{flx/-}$ mice were either used as controls or interbred with mice heterozygous expressing Cre recombinase under control of LysM promoter to generate *Il4ra*$^{\Delta myel}$ mice (23). Of note, LysM-dependent Cre recombinase expression resulted in effective excision of loxP-flanked IL-4 receptor α-chain in bone marrow–derived macrophages (BMDMs) and ATMs validated by decreased responsiveness to IL-4 (Fig. 1).

LysYFP and LysTomato reporter mice were generated by crossing LysM-Cre mice to established Cre reporter mice with loxP-flanked STOP sequence followed by yellow fluorescent protein (YFP) or tdTomato gene inserted into the Gt(ROSA)26Sor locus, which results in tissue-specific fluorophore expression (24–26).

For further analyses *Il4ra*$^{\Delta myel}$ mice were body weight–matched to ensure that findings reflect knockout-dependent effects instead of body weight–dependent effects. Perigonadal white AT (PWAT), s.c. white AT (SWAT), and brown AT (BAT), liver, pancreas, spleen, and brain were dissected, weighed and either fixed in zinc formaldehyde (21516-3.75; Polyscience, Warrington, PA) or shock frozen in liquid nitrogen for further examination. All experiments were approved by the local authorities of the state of Saxony (TVV 18/16; Landesdirektion Sachsen, Dienststelle, Leipzig, Germany).

Immunofluorescence and H&E staining

Fixed AT was embedded in paraffin as described previously (19, 27). Sections were incubated overnight at 4°C with primary Abs anti–Mac-2 (1:1000, CL8942AP; Cedarlane, Burlington, ON, Canada;) and antiperilipinA (1:200, ab3526; Abcam, Cambridge, UK), followed by fluorochrome-conjugated secondary Abs (1:200; Invitrogen, Waltham, MA). DAPI (1:10,000, 62248; Thermo Fisher Scientific, Waltham, MA) was used for nuclear staining. Control staining was performed following the same routines without primary Abs. Images were taken using a confocal Leica SPE microscope (Leica, Wetzlar, Germany). Adipocyte size, interstitial macrophages, and crown-like structures (CLS) density were semiautomatically quantified with CellSens Software (Olympus, Hamburg, Germany) as described previously (28). H&E staining was performed following standard routines (27).

Metabolic characterization

Mice were weighed weekly, starting at 5 wk of age until euthanization. Fat and lean mass was determined at an age of 10 and 20 wk by using an EchoMRI700 Instrument (Echo Medical Systems, Houston, TX). At an age of 30 wk, food and water consumption was evaluated for 72 h and the average daily food and water intake was calculated. The i.p. insulin tolerance tests (ipITTs) and i.p. glucose tolerance tests (ipGTTs) were performed at ages of 8 wk (before starting HFD feeding) and 28 wk (after 20 wk of HFD) as described previously (29). For measurements of spontaneous activity (XYZ cage movement), ability to run in a treadmill and average oxygen consumption (VO2) obese mice at 30 wk of age were housed in metabolic chambers (CaloSys V2.1, TSE Systems, Bad Homburg, Germany) for 72 h. Calculations and analyses of energy expenditure were performed as described previously (30).

Analytical procedures

ELISAs to measure insulin, leptin, adiponectin, and C-reactive protein plasma concentrations were performed according to the manufacturers' guidelines by using mouse standards (Insulin/Leptin ELISA; CrystalChem, Downers Grove, IL; Mouse Adiponectin ELISA; AdipoGen Inc, Incheon, South Korea; Mouse C-reactive protein/CRP Quantikine ELISA Kit; R&D Systems, Minneapolis, MN). Plasma concentrations of free fatty acids, triglycerides, total cholesterol, low-density lipoprotein– (LDL) and high-density lipoprotein–cholesterol were analyzed by an automatic chemical analyzer at the Institute of Laboratory Medicine and Clinical Chemistry at the University of Leipzig.

Culture of BMDMs

BMDMs were generated by flushing bone marrow stems cells out of femur and tibia from selected mice. Cells were plated in RPMI-1640 medium (Sigma-Aldrich, R8758; St. Louis, MO) (supplemented with 10% FCS, 1% glutamine, 1% penicillin-streptomycin) on 10-cm petri dishes and differentiated with 20 ng/ml macrophage colony stimulating factor (315-02; PeproTech, Rocky Hill, NJ) for 7–10 d. Subsequently, BMDMs were stimulated with 20 ng/ml recombinant IL-4 (214-14; PeproTech) or recombinant IL-13 (210-13; PeproTech) for 48 h.

Organotypic AT culture and treatments

Organotypic AT culture (AT explants) and the following experiments were performed as described previously (21).

RNA isolation and quantitative real-time PCR analysis

RNA extraction was performed using TRI Reagent solution (15596018; Thermo Fischer Scientific) followed by cDNA-Synthesis with RevertAid H Minus Reverse Transcriptase (EP0451; Thermo Fisher Scientific). mRNA expression of genes was determined in duplicates by using Hot FirePol EvaGreen qPCR Mix Plus (ROX) (31077; Biotium Inc., Hayward, CA) on an Applied Biosystems StepOnePlus Real-Time PCR-Cycler (Applied Biosystems; Waltham, MA). Relative gene expression was normalized to *Ipo8* and calculated using ΔΔCt method by Pfaffl (31).

Flow cytometry analysis

For flow cytometry staining, immediately dissected PWAT or cultured AT explants were digested using collagenase type II (LS0041-76; Worthington Biochemical, Lakewood, NJ). Then, the cell suspension was filtered through a 70-μm mesh. Fc receptors were blocked with anti-CD16/32 (1:100, 14-0161-82; eBioscience, Waltham, MA) for 10 min. Subsequently, cells were incubated with anti–CD45-FITC (1:200, 11-0451-85; eBioscience), anti–F4/80-PE-Cy7 (1:100, 25-4801-82; eBioscience), anti–CD11c-PE (1:100, 12-0114-83; eBioscience), anti–CD206-Alexa Fluor 647 (1:50, MCA 2235A647; AbD Serotec, Kidlington, UK;), anti-CD3–PE-Cy7 (1:100, 100320; BioLegend; San Diego, CA), anti-CD4–PE (1:100, 100512; BioLegend), anti-CD8b–Alexa Fluor 647 (1:100, 126612; BioLegend;), and/or anti-ST2–PE (1:100, 12-9335-82; eBioscience) for 20 min on ice. For cell proliferation assays and detection of intracellular proteins, cells were fixed and permeabilized according to the BrdU flow kit manufacturer's protocol (552598; BD Biosciences, Franklin Lakes, NJ), before incubation with anti-Ki67 primary Ab (SP6, 1:100, KI681C01; DCS Immunoline, Hamburg, Germany) and anti-Foxp3–eFluor450 (1:100, 48-5773-82; eBioscience). To visualize the Ki67 staining, we used goat-anti-rabbit Alexa Fluor 647 (1:200; Invitrogen). To detect intranuclear BrdU, cells were permeabilized and treated with DNase IV (D5025-15KU; Sigma-Aldrich), followed by incubation with anti–BrdU-Alexa Fluor 647 (PRB-1, 1:50; Abcam). 7-Aminoactinomycin D (1:25, 552598; BD Biosciences) was used to differentiate living cells. Fluorescence minus one and isotype controls were carried out for all experiments. Controls were used to gate leukocyte subsets, and for defining $BrdU^+$ and $Ki67^+$ cells (exemplary gating strategies are provided in Supplemental Fig. 1). M1 macrophages were defined as $CD11c^+CD206^-$ or $CD11c^+CD301^-$, whereas M2 macrophages were defined as $CD11c^-CD206^+$ or $CD11c^-CD301^+$.

Flow cytometry was performed on an LSR II (BD Biosciences) equipped with FACSDiva software 8.0. Data analysis was performed with FlowJo software 10.6 (Tree Star; Ashland, OR).

Western blot analysis

Western blot analysis was performed as described earlier (32). Protein extraction was performed using RIPA buffer (50 mM Tris [pH 8], 150 mM NaCl, 1% nonidet P-40, 0.5% sodium deoxycholate, and 0.1% SDS, supplemented

with 1% PMSF and 1% protease inhibitor mixture [1:100, 5871S; Cell Signaling Technology, Danvers, MA]) and then incubated with polyclonal Abs against ARG1 (1:1000, 610708; BD Biosciences) or β-actin (1:2000, 4970; Cell Signaling Technology) overnight at 4°C. Binding Abs were labeled with peroxidase-conjugated anti-mouse (1:10.000, PI-2000; Vector Laboratories, Peterborough, UK) or anti-rabbit IgG secondary Ab (1:20.000, PI-1000; Vector Laboratories) for 2 h at room temperature. The peroxidase reaction was visualized with an ECL kit (Amersham Pharmacia, Freiburg, Germany). Densiometric analysis was performed using Fiji software 2.0 (33).

Statistical analysis

Prism 8.4 software (GraphPad Software, La Jolla, CA) was used to assess statistical significance. Data in graphs and charts are given as means ± SE. Data sets were tested for statistical outliers before testing for normal distribution and statistical significance using Student *t* test or Mann–Whitney *U* test, accordingly. Data sets of biological replicates were analyzed using paired Student *t* or Wilcoxon tests. Comparison of multiple conditions was performed with a one-way ANOVA followed by Dunnett post hoc test. Any p values <0.05 were considered as significant.

Results

Il4ra$^{\Delta myel}$ *mice are sufficient to study effects of IL-4Rα signaling in ATMs*

We started studying the LysM-Cre–mediated knockout efficiency by treating BMDMs of lean female *Il4ra*$^{\Delta myel}$ and control mice with IL-4 to induce ARG1 expression, which revealed a diminished IL-4 response in *Il4ra*$^{\Delta myel}$ BMDMs by ∼75%, compared with control BMDMs (Fig. 1A; data not shown). Next, we verified the sufficient knockout in ATMs by performing IL-4 stimulation of organotypic AT cultures (AT explants), gained from female *Il4ra*$^{\Delta myel}$ and control mice. After 48 h of IL-4 stimulation, the number of M2 and Ki67$^+$ macrophages significantly increased in *Il4ra*$^{flx/-}$ controls as shown before, whereas there was no significant effect on ATMs from *Il4ra*$^{\Delta myel}$ mice (Fig. 1B, 1C) (21). Hence, LysM-Cre–mediated recombination is sufficient to induce a myeloid-specific knockout of *Il4ra* in ATMs, as shown before for other macrophage subsets (22).

We detected no differences in lean mass, whole body fat mass, food intake, energy expenditure or activity parameters between lean or obese *Il4ra*$^{\Delta myel}$ mice and controls (Supplemental Table I). Levels of plasma lipids (triglycerides, cholesterol, high-density lipoprotein–cholesterol, low-density lipoprotein–cholesterol, free fatty acids) and the adipokines leptin and adiponectin as wells as C-reactive protein and insulin were also unaffected by the knockout (Supplemental Table I). However, by comparing the body weight of chow-fed and HFD-fed mice, a slight increase of body weight was detected for HFD-fed *Il4ra*$^{\Delta myel}$ mice (Fig. 1D). Therefore, mice were body weight–matched for subsequent analyses to ensure that our findings reflect knockout-dependent effects instead of body weight–dependent effects.

Lean Il4ra$^{\Delta myel}$ *mice show reduced insulin sensitivity*

For gross orientation, organ weights were compared between chow-fed mice of different sex and genotype. Interestingly, lean male *Il4ra*$^{\Delta myel}$ mice had ∼50% more BAT (Fig. 2A), whereas lean female *Il4ra*$^{\Delta myel}$ mice had ∼30% more PWAT (Fig. 2B) in relation to body weight. To analyze the effects of *Il4ra*$^{\Delta myel}$ knockout on glucose homeostasis, we performed insulin and glucose tolerance tests on lean male mice. In comparison with the *Il4ra*$^{flx/-}$ controls, glucose tolerance was unaffected by the knockout, but lean *Il4ra*$^{\Delta myel}$ mice exhibited a decreased insulin sensitivity, which indicates a deteriorated glucose metabolism (Fig. 2C–F).

Il4ra$^{\Delta myel}$ *deficiency increases percentage of CD8$^+$ AT T cells in lean mice without affecting ATMs*

To evaluate the cause of the reduced insulin sensitivity of lean *Il4ra*$^{\Delta myel}$ mice, we performed flow cytometry analysis of AT leukocytes. Because macrophages play a central role in obesity-associated AT inflammation and contribute to insulin resistance, we first investigated changes in macrophage content and polarization in PWAT of lean mice (8). However, statistically significant changes could not be detected by flow cytometry analysis comparing macrophage subsets in male and female *Il4ra*$^{\Delta myel}$ and control mice (Fig. 3A–C; Supplemental Table I). Fig. 3E shows representative flow cytometry data. Next, we examined BrdU incorporation of ATMs, because IL-4 and IL-13 are potent stimuli of ATM proliferation ex vivo and ATM proliferation seems to occur preferentially in the M2 macrophage population (19, 21). Yet, we did not find differences in BrdU incorporation of ATMs in chow-fed *Il4ra*$^{\Delta myel}$ mice (Fig. 3D).

AT T cells (ATTs) also have a distinct impact on glucose homeostasis and seem to play a major role in recruiting ATMs to PWAT (9). Hence, we investigated changes in the lymphocyte compartment and found a decreased fraction of ATTs in *Il4ra*$^{\Delta myel}$ mice, which was restricted to female mice only (Fig. 3F). In lean males the fraction of total ATTs as well as CD4$^+$ ATTs was unaffected, but we found an increased proportion of CD8$^+$ ATTs and an increased ratio of CD8$^+$ to CD4$^+$ ATTs (Fig. 3G–J), which may explain the reduced insulin sensitivity in lean male *Il4ra*$^{\Delta myel}$ mice.

Additionally, we investigated Th_2 cells (CD45$^+$CD3$^+$CD4$^+$ST2$^+$) and regulatory T cells (CD45$^+$CD3$^+$CD4$^+$Foxp3$^+$), which promote macrophage M2 polarization and protect mice and humans from insulin resistance (34, 35). However, we did not detect any differences in *Il4ra*$^{\Delta myel}$ mice relative to controls (Supplemental Table I).

Minor Cre recombination in ATTs and differential expression in macrophage subsets

The initially reported restriction of Cre expression on cells of the myeloid line has been challenged by several research groups so far (23, 26, 36). Considering our findings regarding ATTs in *Il4ra*$^{\Delta myel}$ mice and because IL-4Rα signaling seems to be part of the differentiation of at least some T cell subsets, we sought to exclude Cre

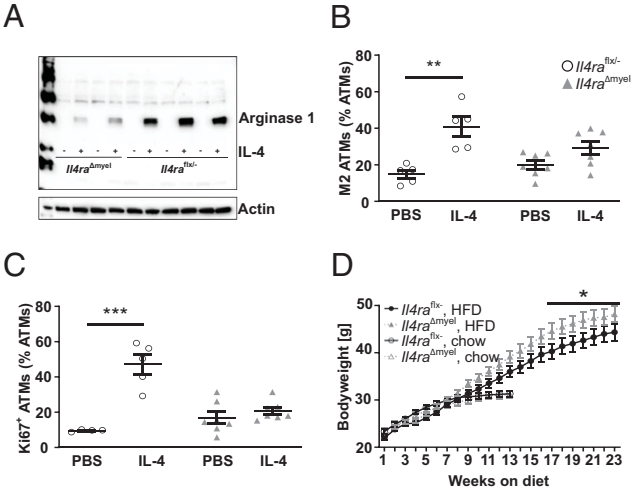

FIGURE 1. Functional verification of *Il4ra* knockout efficiency in ATMs. (**A**) A representative Western blot of ARG1 protein expression in BMDMs derived from female *Il4ra*$^{\Delta myel}$ and controls after IL-4 stimulation (50 ng/ml) for 48 h. (**B** and **C**) Flow cytometry analysis of CD206 und Ki67 expression in ATMs (CD45$^+$F4/80$^+$) of AT explants from male obese mice treated with 50 ng/ml IL-4 for 48 h. (**D**) Body weight of complete *Il4ra*$^{\Delta myel}$ and control cohort on HFD ($n = 22$) and chow diet ($n = 10$). All values are reported as mean ± SEM. Datasets were analyzed for statistical significance using a two-tailed unpaired *t*-test or Mann–Whitney *U* test. $^*p < 0.05$, $^{**}p < 0.01$, $^{***}p < 0.001$.

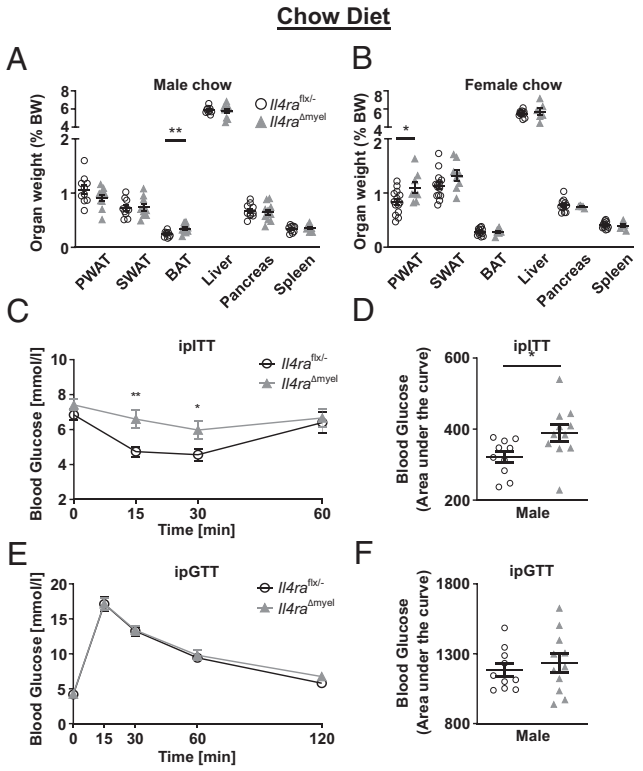

FIGURE 2. Differential AT distribution and reduced insulin sensitivity in lean male *Il4ra*$^{\Delta myel}$ mice. (**A** and **B**) Tissue weights of PWAT, SWAT, BAT, liver, pancreas, and spleen at time of experiments and (**C**–**F**) results of ipITT and ipGTT as absolute values and area under the curve from lean mice (*Il4ra*$^{flx/-}$: $n = 10$; *Il4ra*$^{\Delta myel}$: $n = 11$). All values are reported as mean ± SEM. Datasets were analyzed for statistical significance using a two-tailed unpaired *t* test or Mann–Whitney *U* test. $*p < 0.05$, $**p < 0.01$.

expression in ATTs (37, 38). Using flow cytometry of LysM-Cre mice crossed to two established reporter mouse lines (YFP and TdTomato), we found Cre recombination in 5–20% of T cells ($CD3^+$) cells within PWAT depending on the respective reporter (Supplemental Fig. 2A, 2B). Furthermore, we also examined Cre recombination efficiency in ATMs in PWAT and verified higher reporter protein expression in ATMs, respectively (∼20% YFP^+ ATMs and ∼80% $tdTomato^+$ ATMs; Supplemental Fig. 2A, 2B). Recombination efficiency highly depends on the locus and length of the target gene (39). Importantly, we found a significantly different expression of Cre recombinase in macrophage subsets, favoring M1-polarized ATMs in each model (Supplemental Fig. 2C).

Reduced fasting blood glucose and increased glucose tolerance in Il4ra$^{\Delta myel}$ *mice on HFD*

To investigate the role of IL-4Rα signaling in ATMs in obese AT, we examined male *Il4ra*$^{flx/-}$ and *Il4ra*$^{\Delta myel}$ mice after 20 wk of HFD. We detected no significant differences in body composition (Fig. 4A, Supplemental Table I), but surprisingly, we found parameters of improved glucose homeostasis in *Il4ra*$^{\Delta myel}$ mice on HFD. These mice exhibited a reduced fasting blood glucose and an increased glucose tolerance relative to controls (Fig. 4B–D).

Fewer M1 macrophages in AT of male Il4ra$^{\Delta myel}$ *mice on HFD*

To elucidate the cause of the reported metabolic changes, we examined the composition of macrophage populations in the AT of male *Il4ra*$^{\Delta myel}$ mice on HFD using flow cytometry. Counterintuitively, we found a reduced fraction of M1 macrophages and a reduced M1/M2 ratio in *Il4ra*$^{\Delta myel}$ mice (Fig. 4E–G, 4I), suggesting a lower level of AT inflammation. Yet, we detected no changes regarding ATTs in male *Il4ra*$^{\Delta myel}$ mice on HFD (Supplemental Table I). As in lean mice, we found no effect on ATM proliferation rates in *Il4ra*$^{\Delta myel}$ mice (Fig. 4H).

Male Il4ra$^{\Delta myel}$ *mice on HFD have more interstitial ATMs*

We proceeded by examining markers of adipocyte death and inflammation within AT, which might explain the improved glucose metabolism of male *Il4ra*$^{\Delta myel}$ mice on HFD. After confirming that male *Il4ra*$^{\Delta myel}$ and control mice show no difference in adipocyte size (Supplemental Table I), we determined the incidence of CLS and interstitial macrophages per adipocyte. CLS are clusters of ATMs, which accumulate around dying adipocytes and serve as a marker of adipocyte death and increased inflammatory activity (40, 41). We did not find significantly different numbers of CLS, but the number of interstitial macrophages was augmented in male obese *Il4ra*$^{\Delta myel}$ mice (Fig. 5A–C). Of note, interstitial macrophages are considered to be anti-inflammatory, because they are mostly M2-polarized (40).

Increased Cd206 *gene expression in PWAT of* Il4ra$^{\Delta myel}$ *mice on HFD*

Eventually, we performed gene expression analysis of PWAT from lean and obese *Il4ra*$^{\Delta myel}$ mice. In PWAT of obese male *Il4ra*$^{\Delta myel}$ mice we found an increased expression of *Mrc1* (*Cd206*) compared with control mice also indicating a lower level of AT inflammation in obese *Il4ra*$^{\Delta myel}$ mice (Fig. 5D). Furthermore, we excluded compensatory regulation of cytokines and cytokine receptors that might compromise our model by using relative gene expression analysis of PWAT from lean and obese male *Il4ra*$^{\Delta myel}$ mice (Fig. 5E, 5F, Supplemental Fig. 3A–C).

IL-13 increases CD11c expression in BMDMs and ATMs

IL-13 does not only induce macrophage M2 polarization and macrophage proliferation in AT explants, *Il13* and *Il4ra* are also markedly upregulated in AT of obese mice in vivo, whereas *Il4* is downregulated (16, 21, 42). Therefore, we assume that IL-13 is the prevailing agonist of IL-4Rα in obese AT, which might influence macrophage polarization, because IL-4 and IL-13 have different receptor profiles and trigger slightly different signaling cascades on the same type II IL-4 receptor (43, 44).

To examine why we found fewer M1 macrophages within AT of obese *Il4ra*$^{\Delta myel}$ mice, we stimulated BMDMs of C57Bl6/J and *Il4ra*$^{\Delta myel}$ mice with IL-13 (20 nM) for 48 h and performed gene expression analysis. Unexpectedly, we found a ∼2.7-fold increased *Itgax* (*Cd11c*) expression in C57Bl6/J but not in *Il4ra*$^{\Delta myel}$ mice (Fig. 6A). Subsequently, we stimulated regular AT explants with increasing IL-13 concentrations (1, 10, 50, and 250 nM) for 48 h and examined the effect on ATMs. Using flow cytometry, we found a distinct dose-dependent increase of $CD11c^+$ macrophages, a slight increase of $CD301^+$ macrophages and a marked increase of $CD11c^+CD301^+$ macrophages (Fig. 6B–E). Therefore, we conclude, that IL-13 mainly increases the number of $CD11c^+CD301^+$ macrophages ex vivo and is unexpectedly involved in the upregulation of CD11c protein expression in AT.

Discussion

Macrophage invasion into AT and proinflammatory macrophage activation are important steps in the development of type 2 diabetes during obesity. However, the regulation of macrophage homeostasis in AT and macrophage polarization under lean and obese conditions is not sufficiently understood. To contribute to the understanding of the regulation of ATM polarization and proliferation as well as its

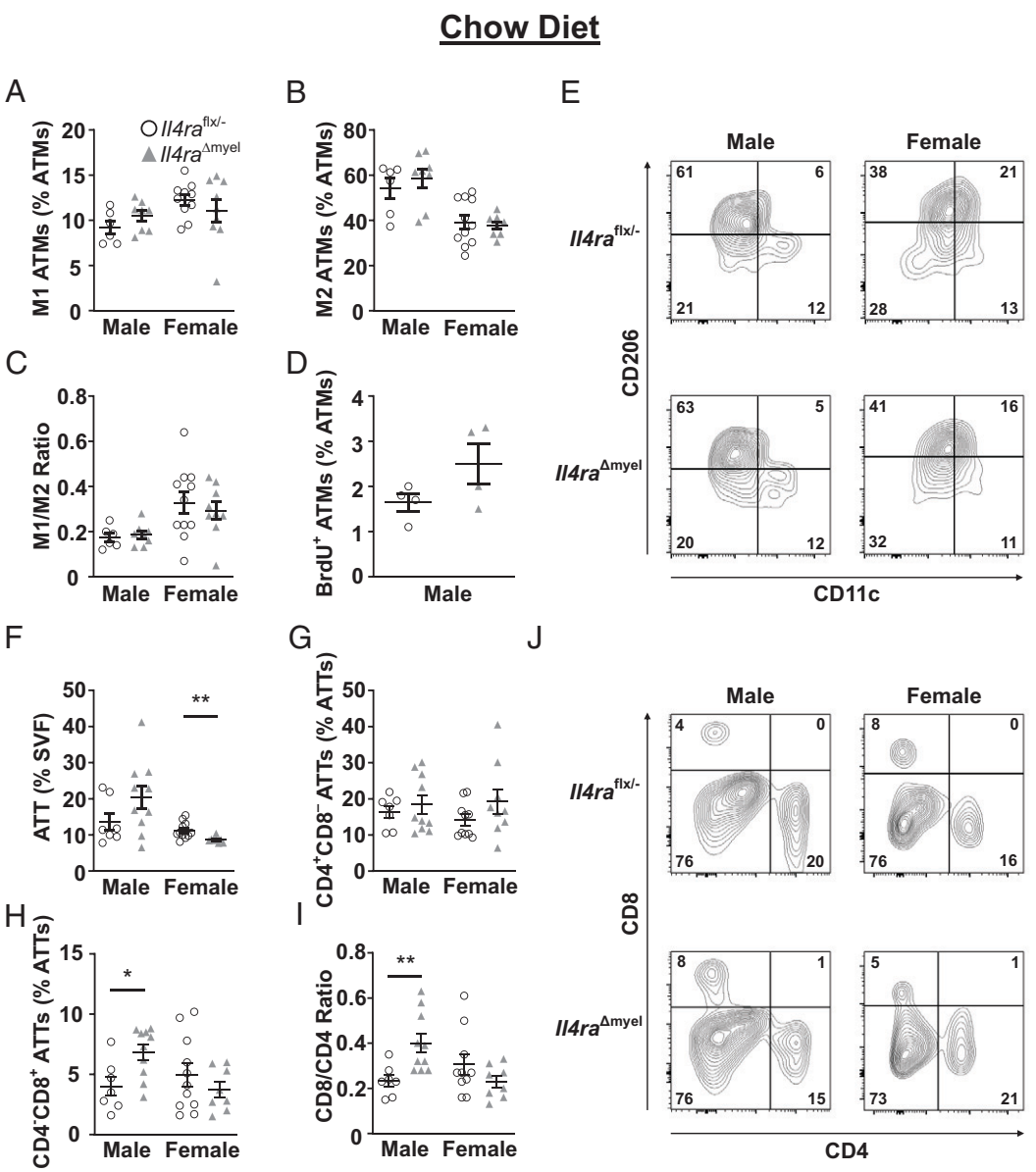

FIGURE 3. Lean *Il4ra*$^{\Delta myel}$ have no alterations in macrophage polarization, but more CD8$^+$ lymphocytes. Flow cytometry analysis of AT leukocytes from lean mice reveals the percentage of (**A**) M1 macrophages (CD45$^+$F4/80$^+$CD11c$^+$CD206$^-$), (**B**) M2 macrophages (CD45$^+$F4/80$^+$CD11c$^-$CD206$^+$), (**D**) and proliferating macrophages (CD45$^+$F4/80$^+$BrdU$^+$) in total macrophages. (**C**) Ratio of M1 to M2 macrophages. (**E**) Representative flow cytometry plots of macrophage subtype discrimination. We also investigated (**F**) ATTs (CD45$^+$CD3$^+$) as percentage of stromal vascular fraction (SVF) and (**G**) CD4$^+$ (CD45$^+$CD3$^+$CD4$^+$CD8$^-$) and (**H**) CD8$^+$ T cells (CD45$^+$CD3$^+$CD4$^+$CD8$^-$) as percentage of overall T cells with flow cytometry. (**I**) Ratio of CD8$^+$ to CD4$^+$ T cells. (**J**) Representative flow cytometry plots of CD4$^+$/CD8$^+$ discrimination. All values are reported as mean ± SEM. Datasets were analyzed for statistical significance using a two-tailed unpaired *t* test or Mann–Whitney *U* test. *$p < 0.05$, **$p < 0.01$.

metabolic consequences, we studied the phenotype of lean and obese *Il4ra*$^{\Delta myel}$ mice.

LysM-Cre–mediated conditional knockout of *Il4ra* resulted in sufficient abrogation of IL-4 signaling in ATMs, well-founded by effective interruption of proliferative and M2-polarizing effects in AT explants. Prior to analysis we excluded obvious brain damage by discontinued IL-4Rα signaling in neurons and relevant Cre recombination in ATTs by flow cytometry analysis of LysYFP and LysTomato reporter mice (26). Furthermore, we investigated the efficiency of Cre recombination in ATMs and ATM subsets. Remarkably, M1 macrophages bear a significantly higher Cre-mediated recombination than M2 macrophages, which should be considered in future research on ATM polarization using LysM-Cre. It should also be noted, that Cre recombination is not exclusive to ATMs, as it also affects dendritic cells and granulocytes (23). Especially, recombination in eosinophilic granulocytes may affect the phenotype of *Il4ra*$^{\Delta myel}$ mice, because these cells seem to represent the main source of IL-4 and IL-13 in AT (45, 46). Although we confirmed the efficiency of our *Il4ra* knockout in AT explants, we cannot exclude effects of soluble IL-4Rα variants on *Il4ra*$^{\Delta myel}$ ATMs (47).

Local macrophage proliferation was initially described by Jenkins et al. (48) as part of type 2 immunity. Our laboratory and others found local proliferation in ATMs and confirmed the influence of IL-4Rα signaling on this process (19, 21, 49). The aim of this study was to substantiate the significance of IL-4Rα signaling on local macrophage proliferation in vivo. However, we were unable to detect any difference in ATM proliferation rates between *Il4ra*$^{\Delta myel}$ mice and controls. These results suggest that IL-4Rα signaling might not be the dominant regulator of ATM proliferation in vivo.

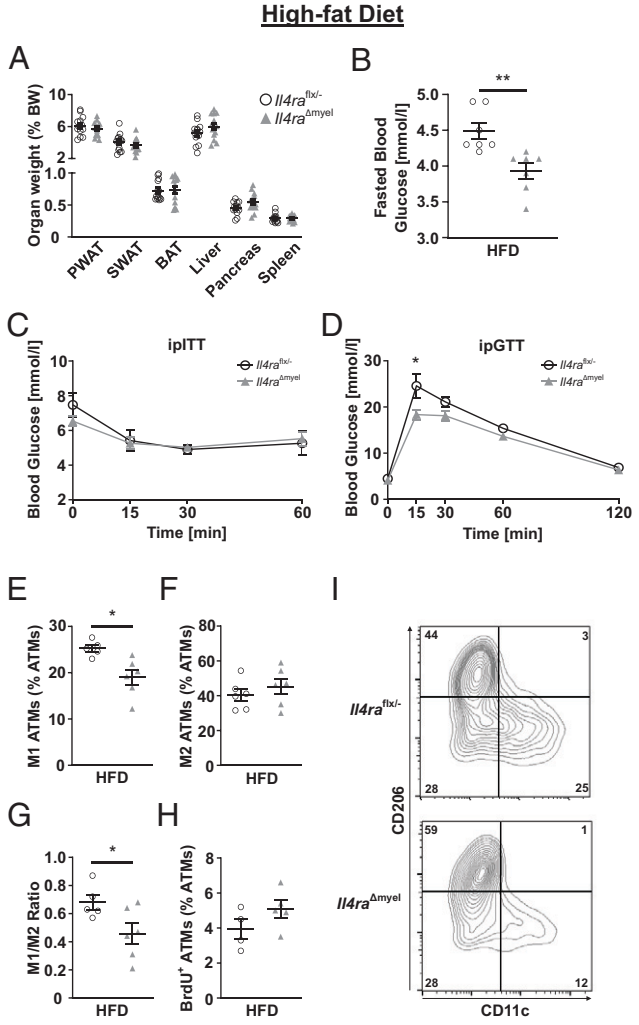

FIGURE 4. Obese male *Il4ra*$^{\Delta myel}$ mice have improved parameters of glucose metabolism and fewer M1 macrophages. (**A**) Tissue weights of PWAT, SWAT, BAT, liver, pancreas, and spleen at time of experiments, (**B**) fasting blood glucose, (**C** and **D**) results of ipITT and ipGTT as absolute values (*Il4ra*$^{flx/-}$: $n = 7$; *Il4ra*$^{\Delta myel}$: $n = 8$). Results of flow cytometry analysis of (**E**) M1 macrophages ($CD45^+F4/80^+CD11c^+CD206^-$), (**F**) M2 macrophages ($CD45^+F4/80^+CD11c^-CD206^+$), (**H**) and proliferating macrophages ($CD45^+F4/80^+BrdU^+$) as percentage of total macrophages. (**G**) Ratio of M1 to M2 macrophages. (**I**) Representative flow cytometry plots of macrophage subtype discrimination. All values are reported as mean ± SEM. Datasets were analyzed for statistical significance using a two-tailed unpaired *t* test or Mann–Whitney *U* test. $*p < 0.05$, $**p < 0.01$.

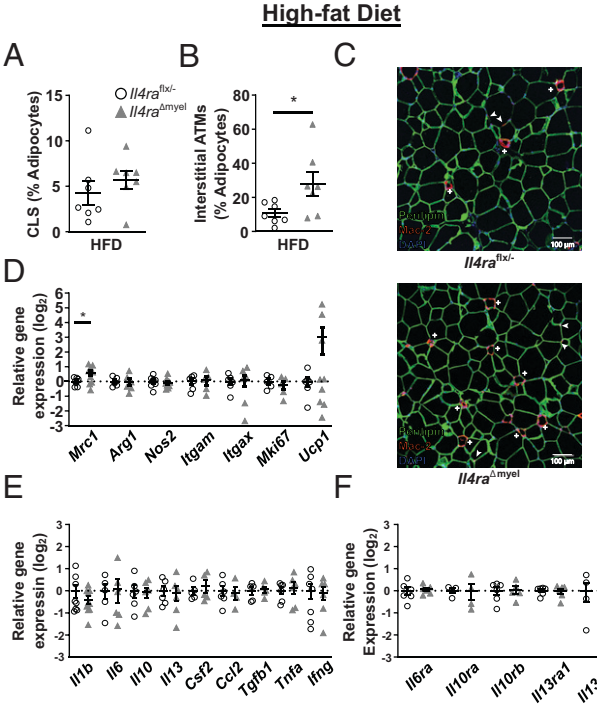

FIGURE 5. Increased number of interstitial macrophages in male *Il4ra*$^{\Delta myel}$ mice on HFD. (**A**) CLS and (**B**) interstitial macrophages per adipocyte as assessed by immunofluorescence staining. (**C**) Representative images of perilipin and Mac-2 immunofluorescence staining with "+" indicating CLS and arrows on interstitial macrophages. Whole AT gene expression analysis of (**D**) macrophage markers, (**E**) different cytokines, (**F**) and their receptors in *Il4ra*$^{\Delta myel}$ mice and controls on HFD. All values are reported as mean ± SEM. Datasets were analyzed for statistical significance using a two-tailed unpaired *t* test or Mann–Whitney *U* test. $*p < 0.05$.

Lean male *Il4ra*$^{\Delta myel}$ mice at 20 wk of age exhibit a reduced insulin sensitivity without changes in the composition of macrophage subsets reflecting the IL-4–independent origin of tissue resident macrophages in lean AT. Instead, the proportion of $CD8^+$ lymphocytes in lean PWAT of male *Il4ra*$^{\Delta myel}$ mice is augmented, resulting in an increased ratio of $CD8^+$ to $CD4^+$ T cells, whereas the overall number of ATTs is unaffected. We assume that the deterioration of insulin sensitivity in lean *Il4ra*$^{\Delta myel}$ mice is part of the early changes during ongoing T cell infiltration in the onset of obesity leading to macrophage accumulation later in time (9). The phenotypic switch of the ATM populations might be pending or disabled by the knockout. The increase of $CD8^+$ T cells may be caused by increased infiltration into AT as suggested by Nishimura et al. or because of local proliferation (9, 50). However, we cannot exclude other knockout-dependent effects influencing $CD8^+$ T cell populations in AT [e.g., by affecting Ag presentation or T cell activation as shown by MHC class II (H2-Ab1) knockout in dendritic cells (51)].

By investigating obese male *Il4ra*$^{\Delta myel}$ mice we detected no changes in the lymphocyte compartment. Instead, we surprisingly found an improved glucose tolerance and a reduction of M1 ($CD11c^+CD206^-$) macrophages in line with a constant M2 ($CD11c^-CD206^+$) population. Even without differences regarding M2 macrophages these results can explain the improved glucose tolerance because the ablation of $CD11c^+$ macrophages normalizes glucose homeostasis in obese mice (13, 14, 40, 52). The unexpected decrease of M1 macrophages, together with an increased *Mrc1* (*Cd206*) gene expression and more interstitial ATMs, indicates a partial protection from AT inflammation in *Il4ra*$^{\Delta myel}$ mice.

To follow up on these findings, we stimulated BMDMs of *Il4ra*$^{\Delta myel}$ mice and controls with IL-13, another agonist of the IL-4Rα, because we assume that IL-13 is the main agonist of IL-4Rα in obese AT because gene expression of *Il13* and *Il4ra* are upregulated, whereas expression of *Il4* is suppressed during AT inflammation (16, 21). Surprisingly, IL-13 stimulation resulted in a strong upregulation of *Itgax* (*Cd11c*) gene expression. To confirm this result in AT, we used our established visceral AT organ culture model and detected an increasing percentage of $CD11c^+$ macrophages after IL-13 stimulation.

Of note, dupilumab, a human mAb to IL-4Rα, is approved in several countries for the treatment of atopic dermatitis, a Th2 cell-driven inflammation. Systemic application of this Ab significantly decreased *ITGAX* gene expression in human skin, indicating a possible translation of our data to humans (53).

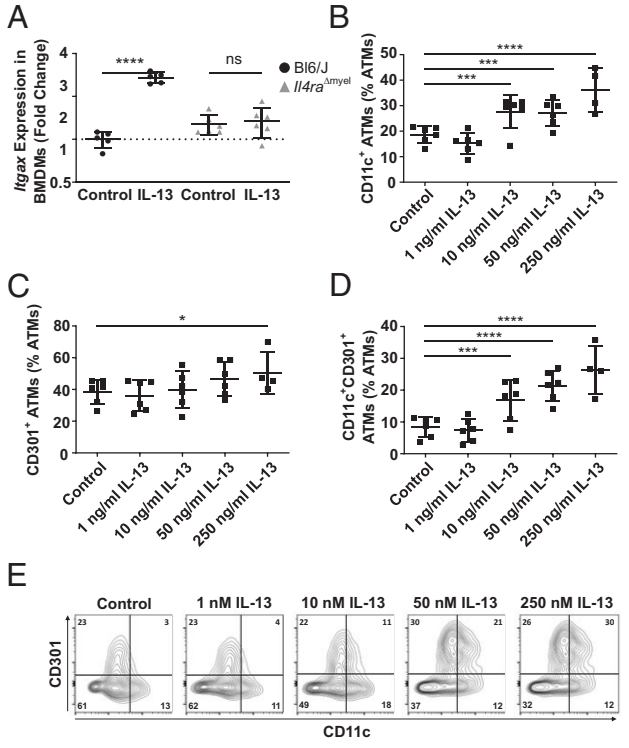

FIGURE 6. IL-4Rα signaling augments *Itgax* gene expression in BMDMs and increases the amount of $CD11c^+$ and $CD11c^+CD206^+$ macrophages in AT explants. (**A**) *Itgax* (*Cd11c*) gene expression in BMDMs of female $Il4ra^{\Delta myel}$ and C57Bl6/J control mice upon stimulation with 20 ng/ml IL-13. (**B**) $CD11c^+$, (**C**) $CD301^+$, and (**D**) $CD11c^+CD301^+$ macrophages as percentage of total macrophages in obese AT explants of male mice after stimulation with different concentrations of IL-13. (**E**) Representative flow cytometry plots of macrophage discrimination in obese AT explants of male mice at increasing IL-13 (1, 10, 50, and 250 nM) concentrations. All values are reported as mean ± SD. Datasets were analyzed for statistical significance using a two-tailed paired *t* test or ANOVA. $*p < 0.05$, $***p < 0.001$, $****p < 0.0001$.

Most of the IL-13–stimulated $CD11c^+$ macrophages were also positive for CD301. Currently, the role of macrophages double positive for M1 and M2 markers in mice is still unclear, but there is evidence for increased parameters of lipid metabolism and a proinflammatory role in human AT inflammation (54). Alternatively, these results may fit into the concept of proinflammatory ATMs that exhibit a less classical activation state, but a so-called metabolically activated phenotype with increased parameters of lipid metabolism (55, 56). Further research regarding $CD11c^+CD301^+$ macrophages and their metabolic phenotype may reveal deeper insights into the function of IL-4Rα signaling in ATMs (57).

Astonishingly, M2 polarization in lean and obese $Il4ra^{\Delta myel}$ mice seems to be unaffected by myeloid cell–specific *Il4ra* knockout. These results raise the question, which mediators, secretion modes or even cell–cell-interactions are the main regulators of M2 polarization of resident tissue macrophages in vivo.

Recent studies show that local and systemic IL-4 or IL-13 administration improves several metabolic parameters in obese mice, but these studies lack insight into AT morphology and especially ATM alterations (15–17, 58). In line with our findings of partial protection from obesity-associated AT inflammation in $Il4ra^{\Delta myel}$ mice Stanya et al. (59) showed that systemic IL-4 administration improves glucose homeostasis by changing hepatic glucose metabolism rather than influencing AT. This conclusion is supported by the results of Youngblood et al. who developed a system for rather local IL-4 application in AT and reported improved fasting blood glucose and glucose tolerance but no significant increase of M1 or M2 macrophages after 2 wk of treatment during HFD (58). Furthermore, IL-4 and IL-13 driven IL-4Rα signaling can increase the proinflammatory response to LPS or *Staphylococcus aureus* by increasing TNF-α and IL-12 production in humans as well as in mice (60, 61). TNF-α and IL-12 serum levels are known to be elevated in obese patients and are mechanistically linked to obesity-induced insulin resistance (62). This supports our findings, because the IL-4Rα-dependent enhancement of TNF-α and IL-12 production may be necessary to sufficiently induce M1 macrophage phenotype during AT inflammation.

Finally, in a mouse model with increased expression of RBP-4 (a retinol transport protein and biomarker for insulin resistance), M2 macrophages are able to activate $CD4^+$ T cells and express high levels of proinflammatory cytokines (63). These CD206-expressing macrophages can thus be considered as proinflammatory, which indicates that alternative activation does not necessarily result in anti-inflammatory action.

However, IL-4 and IL-13 are typically used to induce macrophage M2 polarization in vitro and are considered to be the main regulator for M2 polarization in AT (12, 44). In this study we show, that lean $Il4ra^{\Delta myel}$ mice have a deteriorated insulin sensitivity and more $CD8^+$ T cells in PWAT. In contrast, obese $Il4ra^{\Delta myel}$ mice surprisingly have fewer M1 macrophages in AT and a rather improved metabolic phenotype. Additionally, we show that neither the number of M2 macrophages nor local ATM proliferation are significantly reduced in AT of lean or obese $Il4ra^{\Delta myel}$ mice. In summary, we conclude that obese $Il4ra^{\Delta myel}$ mice are partially protected from AT inflammation. These results can be explained by the unexpected ability of IL-13 to increase the number of M1-like macrophages.

Acknowledgments

We thank Christine Fröhlich of the Martin-Luther University Halle/Wittenberg for teaching and technical assistance. We also thank Andreas Lösche and Kathrin Jäger of the FACS core unit at the University of Leipzig and Nora Raulien of the Martin-Luther University Halle/Wittenberg for consultation and discussion.

Disclosures

The authors have no financial conflicts of interest.

References

1. Tremmel, M., U.-G. Gerdtham, P. M. Nilsson, and S. Saha. 2017. Economic burden of obesity: A systematic literature review. *Int. J. Environ. Res. Public Health* 14: 435–452.
2. Afshin, A., M. H. Forouzanfar, M. B. Reitsma, P. Sur, K. Estep, A. Lee, L. Marczak, A. H. Mokdad, M. Moradi-Lakeh, M. Naghavi, et al; GBD 2015 Obesity Collaborators. 2017. Health effects of overweight and obesity in 195 countries over 25 years. *N. Engl. J. Med.* 377: 13–27.
3. Kolotkin, R. L., and J. R. Andersen. 2017. A systematic review of reviews: exploring the relationship between obesity, weight loss and health-related quality of life. *Clin. Obes.* 7: 273–289.
4. James, W. P. T. 2008. WHO recognition of the global obesity epidemic. *Int. J. Obes.* 32(S7, Suppl 7) S120–S126.
5. Falagas, M. E., and M. Kompoti. 2006. Obesity and infection. *Lancet Infect. Dis.* 6: 438–446.
6. Anandacoomarasamy, A., I. Caterson, P. Sambrook, M. Fransen, and L. March. 2008. The impact of obesity on the musculoskeletal system. *Int. J. Obes.* 32: 211–222.
7. Hotamisligil, G. S., N. S. Shargill, and B. M. Spiegelman. 1993. Adipose expression of tumor necrosis factor-alpha: direct role in obesity-linked insulin resistance. *Science* 259: 87–91.
8. Weisberg, S. P., D. McCann, M. Desai, M. Rosenbaum, R. L. Leibel, and A. W. Ferrante, Jr. 2003. Obesity is associated with macrophage accumulation in adipose tissue. *J. Clin. Invest.* 112: 1796–1808.
9. Nishimura, S., I. Manabe, M. Nagasaki, K. Eto, H. Yamashita, M. Ohsugi, M. Otsu, K. Hara, K. Ueki, S. Sugiura, et al. 2009. CD8+ effector T cells contribute to macrophage recruitment and adipose tissue inflammation in obesity. *Nat. Med.* 15: 914–920.

10. Xu, H., G. T. Barnes, Q. Yang, G. Tan, D. Yang, C. J. Chou, J. Sole, A. Nichols, J. S. Ross, L. A. Tartaglia, and H. Chen. 2003. Chronic inflammation in fat plays a crucial role in the development of obesity-related insulin resistance. *J. Clin. Invest.* 112: 1821–1830.
11. Klöting, N., M. Fasshauer, A. Dietrich, P. Kovacs, M. R. Schön, M. Kern, M. Stumvoll, and M. Blüher. 2010. Insulin-sensitive obesity. *Am. J. Physiol. Endocrinol. Metab.* 299: E506–E515.
12. Russo, L., and C. N. Lumeng. 2018. Properties and functions of adipose tissue macrophages in obesity. *Immunology* 155: 407–417.
13. Patsouris, D., P.-P. Li, D. Thapar, J. Chapman, J. M. Olefsky, and J. G. Neels. 2008. Ablation of CD11c-positive cells normalizes insulin sensitivity in obese insulin resistant animals. *Cell Metab.* 8: 301–309.
14. Wu, H., X. D. Perrard, Q. Wang, J. L. Perrard, V. R. Polsani, P. H. Jones, C. W. Smith, and C. M. Ballantyne. 2010. CD11c expression in adipose tissue and blood and its role in diet-induced obesity. *Arterioscler. Thromb. Vasc. Biol.* 30: 186–192.
15. Chang, Y.-H., K.-T. Ho, S.-H. Lu, C.-N. Huang, and M.-Y. Shiau. 2011. Regulation of glucose/lipid metabolism and insulin sensitivity by interleukin-4. *Int. J. Obes.* 36: 993–998.
16. Kwon, H., S. Laurent, Y. Tang, H. Zong, P. Vemulapalli, and J. E. Pessin. 2014. Adipocyte-specific IKKβ signaling suppresses adipose tissue inflammation through an IL-13-dependent paracrine feedback pathway. *Cell Rep.* 9: 1574–1583.
17. Lin, S.-Y., C.-P. Yang, Y.-Y. Wang, C.-W. Hsiao, W.-Y. Chen, S.-L. Liao, Y.-L. Lo, Y.-H. Chang, C.-J. Hong, and C.-J. Chen. 2020. Interleukin-4 improves metabolic abnormalities in leptin-deficient and high-fat diet mice. *Int. J. Mol. Sci.* 21: 4451.
18. Van Dyken, S. J., and R. M. Locksley. 2013. Interleukin-4- and interleukin-13-mediated alternatively activated macrophages: roles in homeostasis and disease. *Annu. Rev. Immunol.* 31: 317–343.
19. Haase, J., U. Weyer, K. Immig, N. Klöting, M. Blüher, J. Eilers, I. Bechmann, and M. Gericke. 2014. Local proliferation of macrophages in adipose tissue during obesity-induced inflammation. *Diabetologia* 57: 562–571.
20. Amano, S. U., J. L. Cohen, P. Vangala, M. Tencerova, S. M. Nicoloro, J. C. Yawe, Y. Shen, M. P. Czech, and M. Aouadi. 2014. Local proliferation of macrophages contributes to obesity-associated adipose tissue inflammation. *Cell Metab.* 19: 162–171.
21. Braune, J., U. Weyer, C. Hobusch, J. Mauer, J. C. Brüning, I. Bechmann, and M. Gericke. 2017. Il-6 regulates m2 polarization and local proliferation of adipose tissue macrophages in obesity. *J. Immunol.* 198: 2927–2934.
22. Herbert, D. R., C. Hölscher, M. Mohrs, B. Arendse, A. Schwegmann, M. Radwanska, M. Leeto, R. Kirsch, P. Hall, H. Mossmann, et al. 2004. Alternative macrophage activation is essential for survival during schistosomiasis and downmodulates T helper 1 responses and immunopathology. *Immunity* 20: 623–635.
23. Clausen, B. E., C. Burkhardt, W. Reith, R. Renkawitz, and I. Förster. 1999. Conditional gene targeting in macrophages and granulocytes using LysMcre mice. *Transgenic Res.* 8: 265–277.
24. Srinivas, S., T. Watanabe, C. S. Lin, C. M. William, Y. Tanabe, T. M. Jessell, and F. Costantini. 2001. Cre reporter strains produced by targeted insertion of EYFP and ECFP into the ROSA26 locus. *BMC Dev. Biol.* 1: 4.
25. Madisen, L., T. A. Zwingman, S. M. Sunkin, S. W. Oh, H. A. Zariwala, H. Gu, L. L. Ng, R. D. Palmiter, M. J. Hawrylycz, A. R. Jones, et al. 2010. A robust and high-throughput Cre reporting and characterization system for the whole mouse brain. *Nat. Neurosci.* 13: 133–140.
26. Orthgiess, J., M. Gericke, K. Immig, A. Schulz, J. Hirrlinger, I. Bechmann, and J. Eilers. 2016. Neurons exhibit Lyz2 promoter activity in vivo: implications for using LysM-Cre mice in myeloid cell research. *Eur. J. Immunol.* 46: 1529–1532.
27. Berry, R., C. D. Church, M. T. Gericke, E. Jeffery, L. Colman, and M. S. Rodeheffer. 2014. Imaging of adipose tissue. *Methods Enzymol.* 537: 47–73.
28. du Plessis, J., J. van Pelt, H. Korf, C. Mathieu, B. van der Schueren, M. Lannoo, T. Oyen, B. Topal, G. Fetter, S. Nayler, et al. 2015. Association of adipose tissue inflammation with histologic severity of nonalcoholic fatty liver disease. *Gastroenterology* 149: 635–48.e14.
29. Klöting, N., L. Koch, T. Wunderlich, M. Kern, K. Ruschke, W. Krone, J. C. Brüning, and M. Blüher. 2008. Autocrine IGF-1 action in adipocytes controls systemic IGF-1 concentrations and growth. *Diabetes* 57: 2074–2082.
30. Tschöp, M. H., J. R. Speakman, J. R. S. Arch, J. Auwerx, J. C. Brüning, L. Chan, R. H. Eckel, R. V. Farese, Jr., J. E. Galgani, C. Hambly, et al. 2011. A guide to analysis of mouse energy metabolism. *Nat. Methods* 9: 57–63.
31. Pfaffl, M. W. 2001. A new mathematical model for relative quantification in real-time RT-PCR. *Nucleic Acids Res.* 29: e45.
32. Gericke, M. T., J. Kosacka, D. Koch, M. Nowicki, T. Schröder, A. M. Ricken, K. Nieber, and K. Spanel-Borowski. 2009. Receptors for NPY and PACAP differ in expression and activity during adipogenesis in the murine 3T3-L1 fibroblast cell line. *Br. J. Pharmacol.* 157: 620–632.
33. Schindelin, J., I. Arganda-Carreras, E. Frise, V. Kaynig, M. Longair, T. Pietzsch, S. Preibisch, C. Rueden, S. Saalfeld, B. Schmid, et al. 2012. Fiji: an open-source platform for biological-image analysis. *Nat. Methods* 9: 676–682.
34. Feuerer, M., L. Herrero, D. Cipolletta, A. Naaz, J. Wong, A. Nayer, J. Lee, A. B. Goldfine, C. Benoist, S. Shoelson, and D. Mathis. 2009. Lean, but not obese, fat is enriched for a unique population of regulatory T cells that affect metabolic parameters. *Nat. Med.* 15: 930–939.
35. Winer, S., Y. Chan, G. Paltser, D. Truong, H. Tsui, J. Bahrami, R. Dorfman, Y. Wang, J. Zielenski, F. Mastronardi, et al. 2009. Normalization of obesity-associated insulin resistance through immunotherapy. *Nat. Med.* 15: 921–929.
36. Ye, M., H. Iwasaki, C. V. Laiosa, M. Stadtfeld, H. Xie, S. Heck, B. Clausen, K. Akashi, and T. Graf. 2003. Hematopoietic stem cells expressing the myeloid lysozyme gene retain long-term, multilineage repopulation potential. *Immunity* 19: 689–699.
37. Yamashita, M., M. Katsumata, M. Iwashima, M. Kimura, C. Shimizu, T. Kamata, T. Shin, N. Seki, S. Suzuki, M. Taniguchi, and T. Nakayama. 2000. T cell receptor-induced calcineurin activation regulates T helper type 2 cell development by modifying the interleukin 4 receptor signaling complex. *J. Exp. Med.* 191: 1869–1879.
38. Weinreich, M. A., O. A. Odumade, S. C. Jameson, and K. A. Hogquist. 2010. T cells expressing the transcription factor PLZF regulate the development of memory-like CD8+ T cells. *Nat. Immunol.* 11: 709–716.
39. Van Hove, H., A. R. P. Antunes, K. De Vlaminck, I. Scheyltjens, J. A. Van Ginderachter, and K. Movahedi. 2020. Identifying the variables that drive tamoxifen-independent CreERT2 recombination: Implications for microglial fate mapping and gene deletions. *Eur. J. Immunol.* 50: 459–463.
40. Lumeng, C. N., J. B. DelProposto, D. J. Westcott, and A. R. Saltiel. 2008. Phenotypic switching of adipose tissue macrophages with obesity is generated by spatiotemporal differences in macrophage subtypes. *Diabetes* 57: 3239–3246.
41. Cinti, S., G. Mitchell, G. Barbatelli, I. Murano, E. Ceresi, E. Faloia, S. Wang, M. Fortier, A. S. Greenberg, and M. S. Obin. 2005. Adipocyte death defines macrophage localization and function in adipose tissue of obese mice and humans. *J. Lipid Res.* 46: 2347–2355.
42. Zheng, C., Q. Yang, C. Xu, P. Shou, J. Cao, M. Jiang, Q. Chen, G. Cao, Y. Han, F. Li, et al. 2015. CD11b regulates obesity-induced insulin resistance via limiting alternative activation and proliferation of adipose tissue macrophages. *Proc. Natl. Acad. Sci. USA* 112: E7239–E7248.
43. Heller, N. M., X. Qi, I. S. Junttila, K. A. Shirey, S. N. Vogel, W. E. Paul, and A. D. Keegan. 2008. Type I IL-4Rs selectively activate IRS-2 to induce target gene expression in macrophages. *Sci. Signal.* 1: ra17.
44. Kang, K., S. M. Reilly, V. Karabacak, M. R. Gangl, K. Fitzgerald, B. Hatano, and C.-H. Lee. 2008. Adipocyte-derived Th2 cytokines and myeloid PPARdelta regulate macrophage polarization and insulin sensitivity. *Cell Metab.* 7: 485–495.
45. Wu, D., A. B. Molofsky, H.-E. Liang, R. R. Ricardo-Gonzalez, H. A. Jouihan, J. K. Bando, A. Chawla, and R. M. Locksley. 2011. Eosinophils sustain adipose alternatively activated macrophages associated with glucose homeostasis. *Science* 332: 243–247.
46. McCubbrey, A. L., K. C. Allison, A. B. Lee-Sherick, C. V. Jakubzick, and W. J. Janssen. 2017. Promoter specificity and efficacy in conditional and inducible transgenic targeting of lung macrophages. *Front. Immunol.* 8: 1618.
47. Mosley, B., M. P. Beckmann, C. J. March, R. L. Idzerda, S. D. Gimpel, T. VandenBos, D. Friend, A. Alpert, D. Anderson, J. Jackson, et al. 1989. The murine interleukin-4 receptor: molecular cloning and characterization of secreted and membrane bound forms. *Cell* 59: 335–348.
48. Jenkins, S. J., D. Ruckerl, P. C. Cook, L. H. Jones, F. D. Finkelman, N. van Rooijen, A. S. MacDonald, and J. E. Allen. 2011. Local macrophage proliferation, rather than recruitment from the blood, is a signature of TH2 inflammation. *Science* 332: 1284–1288.
49. Zheng, C., Q. Yang, J. Cao, N. Xie, K. Liu, P. Shou, F. Qian, Y. Wang, and Y. Shi. 2016. Local proliferation initiates macrophage accumulation in adipose tissue during obesity. *Cell Death Dis.* 7: e2167.
50. Jiang, E., X. D. Perrard, D. Yang, I. M. Khan, J. L. Perrard, C. W. Smith, C. M. Ballantyne, and H. Wu. 2014. Essential role of CD11a in CD8+ T-cell accumulation and activation in adipose tissue. *Arterioscler. Thromb. Vasc. Biol.* 34: 34–43.
51. Porsche, C. E., J. B. Delproposto, E. Patrick, B. F. Zamarron, and C. N. Lumeng. 2020. Adipose tissue dendritic cell signals are required to maintain T cell homeostasis and obesity-induced expansion. *Mol. Cell. Endocrinol.* 505: 110740.
52. Lumeng, C. N., J. L. Bodzin, and A. R. Saltiel. 2007. Obesity induces a phenotypic switch in adipose tissue macrophage polarization. *J. Clin. Invest.* 117: 175–184.
53. Hamilton, J. D., M. Suárez-Fariñas, N. Dhingra, I. Cardinale, X. Li, A. Kostic, J. E. Ming, A. R. Radin, J. G. Krueger, N. Graham, et al. 2014. Dupilumab improves the molecular signature in skin of patients with moderate-to-severe atopic dermatitis. *J. Allergy Clin. Immunol.* 134: 1293–1300.
54. Wentworth, J. M., G. Naselli, W. A. Brown, L. Doyle, B. Phipson, G. K. Smyth, M. Wabitsch, P. E. O'Brien, and L. C. Harrison. 2010. Pro-inflammatory CD11c+CD206+ adipose tissue macrophages are associated with insulin resistance in human obesity. *Diabetes* 59: 1648–1656.
55. Xu, X., A. Grijalva, A. Skowronski, M. van Eijk, M. J. Serlie, and A. W. Ferrante, Jr. 2013. Obesity activates a program of lysosomal-dependent lipid metabolism in adipose tissue macrophages independently of classic activation. *Cell Metab.* 18: 816–830.
56. Kratz, M., B. R. Coats, K. B. Hisert, D. Hagman, V. Mutskov, E. Peris, K. Q. Schoenfelt, J. N. Kuzma, I. Larson, P. S. Billing, et al. 2014. Metabolic dysfunction drives a mechanistically distinct proinflammatory phenotype in adipose tissue macrophages. *Cell Metab.* 20: 614–625.
57. Vats, D., L. Mukundan, J. I. Odegaard, L. Zhang, K. L. Smith, C. R. Morel, R. A. Wagner, D. R. Greaves, P. J. Murray, and A. Chawla. 2006. Oxidative metabolism and PGC-1beta attenuate macrophage-mediated inflammation. [Published erratum appears in 2006 *Cell Metab.* 4: 255.] *Cell Metab.* 4: 13–24.
58. Youngblood, R., C. G. Flesher, J. Delproposto, N. A. Baker, C. K. Neeley, F. Li, C. N. Lumeng, L. D. Shea, and R. W. O'Rourke. 2020. Regulation of adipose tissue inflammation and systemic metabolism in murine obesity by polymer

implants loaded with lentiviral vectors encoding human interleukin-4. *Biotechnol. Bioeng.* 117: 3891–3901.
59. Stanya, K. J., D. Jacobi, S. Liu, P. Bhargava, L. Dai, M. R. Gangl, K. Inouye, J. L. Barlow, Y. Ji, J. P. Mizgerd, et al. 2013. Direct control of hepatic glucose production by interleukin-13 in mice. *J. Clin. Invest.* 123: 261–271.
60. D'Andrea, A., X. Ma, M. Aste-Amezaga, C. Paganin, and G. Trinchieri. 1995. Stimulatory and inhibitory effects of interleukin (IL)-4 and IL-13 on the production of cytokines by human peripheral blood mononuclear cells: priming for IL-12 and tumor necrosis factor alpha production. *J. Exp. Med.* 181: 537–546.PubMed
61. Roy, S., R. Charboneau, D. Melnyk, and R. A. Barke. 2000. Interleukin-4 regulates macrophage interleukin-12 protein synthesis through a c-fos mediated mechanism. *Surgery* 128: 219–224.
62. Schmidt, F. M., J. Weschenfelder, C. Sander, J. Minkwitz, J. Thormann, T. Chittka, R. Mergl, K. C. Kirkby, M. Faßhauer, M. Stumvoll, et al. 2015. Inflammatory cytokines in general and central obesity and modulating effects of physical activity. *PLoS One* 10: e0121971.
63. Moraes-Vieira, P. M., A. Castoldi, P. Aryal, K. Wellenstein, O. D. Peroni, and B. B. Kahn. 2016. Antigen presentation and t-cell activation are critical for rbp4-induced insulin resistance. *Diabetes* 65: 1317–1327.